IMPROVING CONTENT-BASED TARGET AND CHANGE DETECTION IN ALOS PALSAR IMAGES WITH EFFICIENT FEATURE SELECTION

Matthieu Molinier[(1)(2)], Ville Viitaniemi[(2)], Markus Koskela[(2)], Jorma Laaksonen[(2)], Yrjö Rauste[(1)], Anne Lönnqvist[(1)], and Tuomas Häme[(1)]

[(1)]*VTT Technical Research Centre of Finland, Digital Information Systems, P.O. Box 1000 - VM3, FI-02044 VTT, Finland, Email: firstname.lastname@vtt.fi*
[(2)]*Helsinki University of Technology, Department of Information and Computer Science, P.O. Box 5400, FI-02015 TKK, Finland, Email: firstname.lastname@hut.fi*

ABSTRACT

Self-Organising Maps (SOMs) have been successfully applied to content-based image retrieval (CBIR). In this study, we investigate the potential of PicSOM, an image database browsing system, applied to quad-polarised ALOS PALSAR images. Databases of small images were artificially created, either from a single satellite image for object detection, or two satellite images when considering change detection. Polarimetric features were extracted from the images to allow image indexing. By querying the databases, it was possible to detect target classes, as well as changes between the two images. Results open a full range of applications, from structure detection to change detection, to be embedded in a same operative system. The framework may be particularly suitable for long-term monitoring of strategic sites.

Key words: content-based information retrieval, self-organising maps, high resolution satellite images, polarimetric spaceborne SAR, change detection.

1. INTRODUCTION

Three latest generation SAR satellites have been launched - ALOS PALSAR, TerraSAR-X and Radarsat-2. The availability of dual-polarisation and fully polarimetric data, instead of earlier single-polarisation data, will enable a deeper analysis of backscattering processes and thereby pave the way for many new applications of spaceborne SAR data. At the same time, these satellite missions generate a huge amount of data at a higher resolution than previous spaceborne SAR sensors.

Current Earth Observation archiving systems typically support queries by sensor type, acquisition date, imagery coverage or a combination of them. Concurrently, security-concerned applications relying on satellite imagery often demand repeated or continuous monitoring, and intelligent access to the extracted information. There is therefore a growing interest in the remote sensing community to access databases directly by the information contained in images. Content-based image retrieval (CBIR) allows management of large image archives [1–6], as well as satellite image annotation and interpretation [2, 7–9].

Our work extends and improves the potential of PicSOM, a CBIR system based on Self-Organising Maps (SOMs), for remote sensing image analysis [10]. In the PicSOM image database browsing system [11], several thousands of images are mapped onto Self-Organising Maps (SOMs) [12], through the extraction of image descriptors including textural and color features. After the SOMs are trained, the user can visually query the database and the system automatically finds images similar to those selected. This approach has been successfully applied to databases of conventional images [13, 14] as well as man-made structure and change detection in high-resolution satellite optical images [10].

This article presents our latest experiments with PicSOM on a spaceborne polarimetric ALOS PALSAR dataset. The key idea of our study, first presented at ESA-EUSC 2005 conference [15], is to artificially generate a database of small images (or *imagelets*) from each full satellite image to be analysed. PicSOM can be trained on that virtual database, then queried for finding objects of interest. Imagelets can be extracted for the detection of man-made structures or other targets, or to detect changes if two scenes are available.

The data consists of two fully polarimetric scenes acquired in March and May 2007 over Kuortane, in central Finland. Typically, a scene was divided into several thousands of imagelets of size 16×16 pixels. We have extended PicSOM to include widely used polarimetric features (e.g. co-polarised and cross-polarised ra-

tios, among many others). Polarimetric features extracted pixel by pixel were grouped into imagelet-wise feature vectors in several ways, including averaging and histograms by vector quantisation. Evaluation of the methods for feature selection were provided using classification images. Change detection was also performed and evaluated versus a reference change map and ground truth of clearcuts obtained from the local forest administration of Kuortane. Potential applications of this work are high-resolution satellite image annotation, or monitoring of sensitive areas for undeclared human activity, both in an interactive way.

2. DATA AND PRE-PROCESSING

2.1. Satellite imagery

Two quad-polarised ALOS PALSAR images were acquired on 29th March 2007 and 14th of May 2007 over Kuortane, in central Finland (62°48'33"N, 23°30'50"E). The off-nadir angle was 21.5 degrees and incidence angle 24 degrees. The fully polarimetric scenes cover an area of 35km wide and 70km long. The were incoherently averaged into 6-look images in the Stokes matrix domain. Although Kuortane area is relatively flat (elevation 38-230 m), the original scenes were rectified using a Digital Elevation Model. Rectified 6-look data had a resolution of 25m in both azimuth and range. The refined Lee speckle filter [16] was applied with window size 3x3 pixels to reduce noise.

Kuortane area is dominated with small areas of different land cover types [17]. There are a few built-up areas but these mostly belong to discontinuous fabric of individual single family houses. Built-up areas contain lots of mature trees. The dominant soil type is glacial drift, but sand areas exist also. Coniferous forest on mineral soil is the dominating forest type, second type being mixed forests on mineral soil.

In the March scene, the lakes were covered with ice and some floating water on top of it. The ice was totally melt in the May scene. Fig. 1 shows the Pauli decomposition of the May image of Kuortane. In this image, power scattered by single or odd-bounce targets ($HH + VV$) is represented in blue (associated with surface scattering - e.g. water or fields), double bounce ($HH - VV$) in red or white (built-up areas) and volume scattering (HV) in green (vegetated areas).

2.2. Database preparation

The whole scenes were considered as the study area. PicSOM image retrieval system typically requires several thousands of images in a database in order to produce relevant indexing. Each image was thus cut into 9241 non-overlapping small images or *imagelets*, of size 16×16 pixels (only imagelets containing actual data and

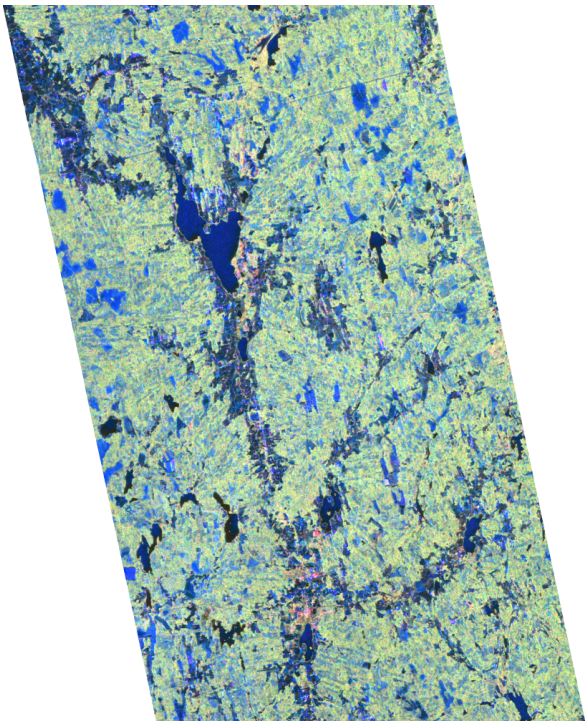

Fig. 1. Pauli decomposition of rectified PALSAR May image over Kuortane, Finland. ©JAXA and METI 2006

no null value resulting from registration procedure were kept). After the splitting into imagelets, the amount of contents in each image is reduced, from many classes in the study scene (bare soil, buildings, forest...) to only a few in each imagelet.

In order to evaluate methods quantitatively [18], a reference image was created by classifying each SAR image with PolSARpro [19] supervised classifier, using 5 land-cover classes $\{$*water, field, forest, marsh, urban*$\}$. Corine Land Cover 2002 data was used to delineate training areas. Average classification accurracy was 80% for both scenes, but it was significantly lower for the urban class (buildings). This is probably because the scenes contain rather sparsely inhabited areas or relatively small buildings. In addition, a reference change image was created using AutoChange [20], an automatic change detection software originally developed for forestry.

3. METHODS

The PicSOM system used in this study has originally been developed for content-based image retrieval (CBIR) research [13, 14, 21]. It is based on using the Self-Organising Map (SOM) [12] as an efficient indexing structure for the images. We show how this same technique might also be applied in the semi-automated, interactive analysis of satellite images.

3.1. Self-Organising Maps

The Self-Organising Map (SOM) [12] is a neurally-motivated unsupervised learning technique, forming a nonlinear mapping of a high-dimensional input space to a typically two-dimensional grid of neural units. During SOM training, the *model vectors* in its neurons get values which form a topology-preserving mapping: neighboring vectors in the input space are mapped into nearby units in the SOM grid. Patterns mutually similar in respect to a feature are closely located on the SOM surface. Training is initialised with random values of model vectors $\mathbf{m}_i$ for each map unit i. For each input sample $\mathbf{x}(t)$, the "winner" or *best-matching* map unit (BMU) $c(\mathbf{x})$ is identified on the map by the condition

$$\forall i: \quad \|\mathbf{x}(t) - \mathbf{m}_{c(\mathbf{x})}(t)\| \leq \|\mathbf{x}(t) - \mathbf{m}_i(t)\| \,, \qquad (1)$$

where $\|\cdot\|$ is commonly the Euclidean metric. After finding the BMU, a subset of the model vectors constituting a neighborhood centered around node $c(\mathbf{x})$ are updated as

$$\mathbf{m}_i(t+1) = \mathbf{m}_i(t) + h(t; c(\mathbf{x}), i)(\mathbf{x}(t) - \mathbf{m}_i(t)) \,. \quad (2)$$

with $h(t; c(\mathbf{x}), i)$ a decreasing "neighborhood function" of the distance between the i-th and $c(\mathbf{x})$-th nodes on the map grid. Training is iterated over the available samples, and $h(t; c(\mathbf{x}), i)$ is allowed to decrease in time to guarantee convergence of prototype vectors $\mathbf{m}_i$. After training, all input samples $\mathbf{x}$ are once more mapped to the SOM, each in its BMU. Every SOM unit is then assigned a *visual label* from the imagelet whose feature vector was the nearest to the model vector.

3.2. PicSOM for content-based image retrieval

The PicSOM system [11] implements two essential CBIR techniques, query by examples (QBE) and relevance feedback. These methods can be used for interactive retrieval of any type of visual or non-visual content.

In interactive QBE, the system presents in a visual interface some images to the user, who then marks a subset of them as relevant to the query. This relevance information is fed back to the system, which seeks more similar images and returns them in the next query round. In PicSOM, multiple SOMs are used in parallel, each created with a different low-level visual feature. The different SOMs and their underlying feature extraction schemes impose different similarity functions on the images, allowing PicSOM to adapt to different retrieval tasks.

Relevance feedback has been implemented by using the parallel SOMs. Each image presented in PicSOM is graded by the user as either relevant or non-relevant. All these relevance grades are then projected to the BMUs of the graded images on all SOM surfaces. Maps where there are many relevant images mapped in same or nearby SOM units agree well with the user's conception on the relevance and semantic similarity of the images.

The relevance information placed in the SOM units is spread also to the neighboring units. Each image is given a total qualification value obtained as a sum of the qualification values from its BMUs from the different feature SOM surfaces. Those yet unseen images which have the highest qualification values will then be shown to the user on the next query round. In PicSOM, features that fail to coincide with the user's conceptions always produce lower qualification values than those descriptors that match the user's expectations. More can be found in [10].

As an illustrative example obtained from a satellite optical image, Fig. 2 displays a SOM created from the texture feature [10]. The water regions are mapped into two separate areas due to the different textures of the calm and wavy water surfaces, to bottom right and top left corners of the map, respectively. This demonstrates how PicSOM organises imagelets in the database according to a specific feature.

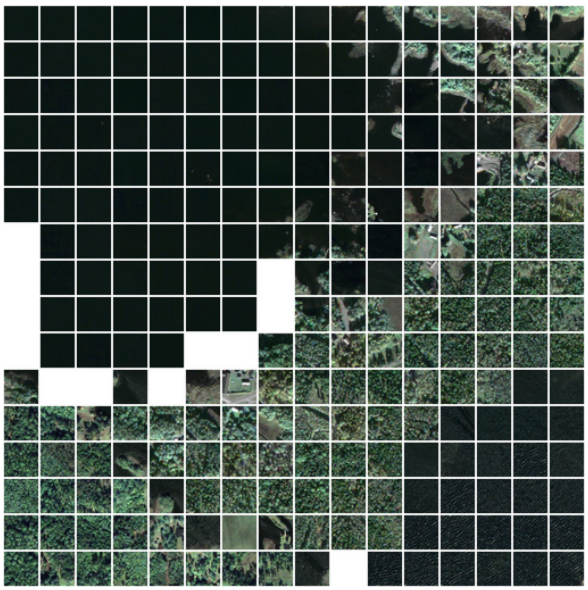

Fig. 2. Organisation of the imagelets by their texture content on a 16×16 SOM surface - original image : Quickbird from western Finland, September 2005 [10]

3.3. Feature extraction

Features have to be extracted from the imagelets to allow their indexing by the Self-Organising Map. The original PicSOM features were developed for RGB optical images. Features used in CBIR usually describe generic image properties, like color distribution, texture or shapes [9].

In the case of polarimetric radar imagery, meaningful polarimetric features have to be considered instead. First the polarimetric features were extracted for each pixel of the full size radar images. Then for each imagelet, the pixel-wise features were grouped in three different ways to form feature vectors representing the imagelet.

3.3.1. Pixel-wise features

Six groups of polarimetric features were extracted from imagelets [18] (citations below refer to example of previous polarimetric studies with those features for a given application) :

BACKSCATTER : the 3 backscattering coefficients in HH, HV and VV polarisations [22–24].

HH-VV : amplitude of correlation between HH and VV channels [23, 24] and phase difference between HH and VV [22, 23].

LOGRATIOS : ratio HV/VV in dB [24], co-polarised and cross-polarised ratios [25].

RATIOS : co-polarisation ratio γ [22] and depolarisation ratio δ [22, 23]

H-A-α : entropy/anisotropy/α angle from the Cloude-Pottier decomposition [26]

TOUZI : 4 discriminators related to the degree of polarisation and extracted from the Mueller matrix [27]

In case of Cloude-Pottier decomposition and Touzi discriminators, the features were extracted from 6-look data in moving windows of 3x3 pixels.

The features were computed for each pixel and stored for later use. In previous studies features were not normalised : we tested normalisation of each vector component to zero mean and unit variance, expecting an improvement comparing to unscaled vectors, especially with the high dynamic range of input PALSAR images.

3.3.2. Imagelet-wise feature vectors

In the experiments we wanted to study how the six basic feature groups could be used most efficiently for analysing the content of the imagelets. Pixel-wise features were grouped into imagelet-wise feature vectors in three different ways :

- the pixel-wise feature values were averaged over the 256 pixels in each imagelet,
- the pixel-wise feature values were averaged per 8×8 pixel blocks - 4 blocks per imagelet,
- histograms were created to describe the distribution of the feature vector values more precisely.

The feature vector histograms were generated as follows. A Self-Organising Map (SOM) of size WxH map units was initialised. One pixel was then randomly picked from the full size image and its feature vector value was used to adapt the SOM. This random selection and adaptation was iterated 10 million times to obtain a trained SOM. The SOM was then used as a codebook or vector quantiser, the tesselation regions of which were used as bins in histogram creation. For each imagelet, the 256 pixel-wise feature vectors were mapped to their nearest map units on the SOM and the total number of hits in each unit or bin constituted the imagelet-wise histogram feature. For comparing the similarity of the histogram features we used the Euclidean distance between them. In the experiments we varied the WxH-size of the SOM used in the histogram feature calculation in order to find an optimal number of histogram bins.

In addition to polarimetric features vectors, a xy-coordinate feature was carried along the whole analysis process. The xy-coordinate feature allowed to keep track of the position of any imagelet within the full image (as row/column indexes), and completed the framework for change detection.

3.3.3. SOM training on feature vectors

In PicSOM, several SOMs are trained in parallel (one per feature). Each feature vector was used 100 times in training (Eqs. (1) and (2)). The map sizes were set to 64×64 units for the visual features SOMs, and 125×125 for the coordinate SOM. There were on the average $9241/4096 \approx 2.25$ imagelets mapped in each map unit of the visual SOMs, and exactly one image location on the coordinate map (units mapping to locations on the registration canvas of the original image were not considered in the SOM).

3.4. PicSOM for target detection

The visual querying presented in early works [10] was not carried out with the PALSAR data, as 16x16 pixel imagelets of Pauli decomposition were not suitable for visual querying based on image content. PicSOM system could however be used to perform automatic detection of target classes. The qualification value assigned to each imagelet by the PicSOM system is a discrimination value, which indicates the likeliness that the specific imagelet belongs to that semantic class (label) [10]. Imagelets can be sorted by decreasing order of similarity to a given class, and a threshold can then be set to retrieve the imagelets most similar to that semantic class. This was done for the 5 semantic classes, and combined to "greedy" sequential forward selection of features.

3.5. Content-based unsupervised change detection

We devised a method for finding pairs of imagelets, one from March image and the other from May, which differed the most in the sense of some of the extracted fea-

tures. Only the true changes in the imagelet's content would then give rise to such a striking change in the feature vector's value that its projection on the SOM surface is moved to a substantially different location. The substantiality of the change can therefore be measured as the distance between the best matching units (BMUs) of the different months' feature vectors on a same SOM.

Imagelet pairs were ordered by descending pair-wise BMU distance on a given feature SOM – the higher the distance, the more substantial change in content occurred. A fixed number of imagelet pairs were then regarded as the locations where the most substantial changes had taken place. Several feature SOMs can be used simultaneously, in which case the pair-wise BMU distances on different SOMs were normalised then combined [10].

4. RESULTS AND DISCUSSION

We divided both SAR images into two parts : the upper part and the lower part. One of the four parts was then in turn used as a training set for creating the models for the 5 landcover classes. By using all the remaining three parts for three different tests, we could obtain performance measures for both intra-image and inter-image generalisation ability. For the latter, we could further distinguish between cases where the training and testing data were from same or different location. In the case of same location we were also able to perform unsupervised change detection between the two images as in [10].

4.1. Performance evaluation of features in retrieval tasks

The results of our first experiment showed that the TOUZI and BACKSCATTER features were the two best ones for both the average and histogram feature types - Tab 1. The mutual order of TOUZI and BACKSCATTER was dependent on the landcover class studied. BACKSCATTER seemed to be the best feature for detecting fields and especially water. However, these two classes were often mixed with each other in the retrieval tasks, so other features should be used to separate them. TOUZI was another good feature overall, and best one for detecting marshes. From the five landcover classes the urban class was found to be the most difficult one to retrieve, as expected. H-A-α seemed to work relatively well for retrieving the urban class.

Our main interest was, however, to find out whether the histogram method or the average method was superior. The results showed that in four cases out of six the histogram method was better.

For each feature and each class, the 10 and 100 most relevant imagelets were retrieved and considered truly relevant if the target class was present in the reference image. The higher the number of truly relevant imagelets, the better the feature or feature combination was - Tab 1.

4.2. Feature selection to improve overall accuracy

In a second experiment we wanted to study which combination of the individual features studied earlier could produce the best total average precision in the PicSOM system. For feature selection, we used the "greedy" sequential forward selection algorithm. The results showed that a proper combination of the best-performing features performed usually better than any of the individual features. This was especially true on the number of truly relevant images retrieved with feature selection compared to any feature alone.

Tab 1 shows the average precision values obtained with the best features for a given target class, and considering several testing schemes. Under each target class row is indicated the number of imagelets containing that class in the reference images and the percentage of total imagelets. The columns *"same"*, *"diff"*, and *"cross"* refer to cases where the test set is either the other half of the same image, the same half of the other image, or the other half of the other image, respectively, than the training set. These are repeated four times, i.e. for the different permutations of the training set, and then averaged. The mean average precision over these three cases is shown in column "mean avg. precision". When looking at the columns *"same"*, *"diff"*, and *"cross"*, results suggest that for a given feature vector, all testing schemes returned similar results, underlining the robustness of the method. For each target class in Tab 1, the feature vector providing the best mean average precision and the highest number of relevant imagelets for 10 or 100 retrieved imagelets are shown in bold. It is clear that feature selection tends to improve the results, for all classes but water in our experiments.

4.3. PicSOM for unsupervised change detection

In the last experiment, we replicated for polarimetric SAR images our earlier studies on optical images in using SOMs for unsupervised change detection [10]. 50, 100, 150 and 300 most relevant imagelets regarding to changes were considered and the results were visually compared to the reference change images.

Compared to the clearcut ground truth, the BACKSCATTER plain feature produced the best result. The stands that have been cut between March and May 2007 around Kuortane represented tiny areas that were challenging to detect with the imagelet method. A significant part of the 50 most relevant imagelets for the BACKSCATTER feature matched some locations of actual clearcuts. It was understandable as the HV backscattering coefficient is strongly linked to biomass index even at L-band. However not all the clearcuts were retrieved, as the imagelet-based approach only retrieve wide changes.

Histograms of LOGRATIOS and POLRATIOS were the best features to retrieve changes over water bodies,

Table 1. Average precision of the best features versus reference classification images, within several training schemes. The columns "rel@10" and "rel@100" refer to the numbers of relevant imagelets found on average among the 10 and 100 first retrieved imagelets given a feature vector.

class	**type**	**mean avg. precision**	*same*	*diff*	*cross*	**rel@10**	**rel@100**	**feature**
field	global avg	0,758	0,771	0,754	0,751	9,25	86,25	BACKSCATTER
21%	4-zone avg	0,730	0,733	0,735	0,722	8,08	83,50	BACKSCATTER
928	histogram	**0,864**	0,878	0,849	0,866	**9,83**	95,42	BACKSCATTER
	feature sel.	**0,864**	0,878	0,851	0,861	**9,83**	**97,83**	
forest	global avg	0,987	0,986	0,987	0,987	**10,00**	99,67	POLRATIOS
82%	4-zone avg	0,985	0,987	0,983	0,985	9,92	99,17	H-A-α
3769	histogram	0,993	0,995	0,992	0,991	**10,00**	99,83	TOUZI
	feature sel.	**0,995**	0,996	0,994	0,994	**10,00**	**100,00**	
marsh	global avg	0,461	0,443	0,465	0,475	6,00	43,50	TOUZI
0,8%	4-zone avg	0,432	0,424	0,439	0,433	6,83	41,58	TOUZI
108	histogram	0,569	0,563	0,579	0,567	7,75	54,67	TOUZI
	feature sel.	**0,633**	0,713	0,590	0,594	**8,25**	**55,50**	
urban	global avg	0,336	0,317	0,357	0,333	4,42	12,50	H-A-α
0,3%	4-zone avg	0,389	0,382	0,401	0,385	4,58	12,75	H-A-α
19	histogram	0,291	0,301	0,324	0,241	3,83	10,83	H-A-α
	feature sel.	**0,428**	0,402	0,468	0,412	**4,92**	**15,33**	
water	global avg	0,877	0,946	0,844	0,841	**10,00**	64,25	BACKSCATTER
2%	4-zone avg	**0,881**	0,902	0,865	0,875	**10,00**	**67,08**	BACKSCATTER
77	histogram	0,527	0,746	0,471	0,363	7,25	42,92	BACKSCATTER
	feature sel.	0,754	0,938	0,656	0,669	9,00	57,92	
overall	global avg	0,684	0,693	0,681	0,677	7,93	61,23	
	4-zone avg	0,683	0,685	0,685	0,680	7,88	60,82	
	histogram	0,649	0,696	0,643	0,606	7,73	60,73	
	feature sel.	**0,735**	0,785	0,712	0,706	**8,40**	**65,32**	

mainly corresponding to ice melting between March and May. Those features are ratio of backscattering coefficients combinations, which change when ice melts - copolarisation and depolarisation ratios have been used in [22, 23] for sea ice classification.

Fig. 3 shows the reference change image obtained with AutoChange, that was used to visually assess the relevance of imagelet selection. We are aware that using the same data for building the reference change image and carrying out change detection experiments is not ideal, but we did not have any other reference data that could have been used for that purpose in dates reasonably close to the acquisition dates of the PALSAR images. It is also to be noticed that changes in water areas do not appear in the AutoChange reference change image.

Fig. 4 shows the resulting selection of 300 most relevant images for change detection using all 25x20 histogram features. The changes in fields on top-left corner and bottom of the image were well retrieved, as well as changes in main water bodies (melting ice, not appearing in the reference change image).

The results of these experiments verified that our change detection technique is also applicable to SAR data even though the higher noise level of SAR data has some negative effect on its accuracy. Imagelet-based structure detection does not provide direct delineation of objects of interest (contrary to pixel-based methods), but it can highlight in a full scene locations with potentially interesting structures or contents.

SOMs that have been trained using previous images can be used in the analysis of new imagery. This approach may be applied in supervised monitoring of strategic sites, i.e. novelty or change detection with two or more images. Such a system could point out locations in the full image where there may be potentially interesting structures, present, appearing or disappearing, and that match features defined visually by the user. One of the many advantages of PicSOM for polarimetric SAR data analysis is its ability to integrate various features, and perform a selection of relevant ones based on user queries. The same framework allows for classification, structure detection, and change detection - in both supervised or unsupervised ways.

5. CONCLUSIONS

We have presented how a content-based image retrieval system, PicSOM, can be used with polarimetric SAR images for tasks like target class retrieval, as well as change detection. The approach relies on the decompo-

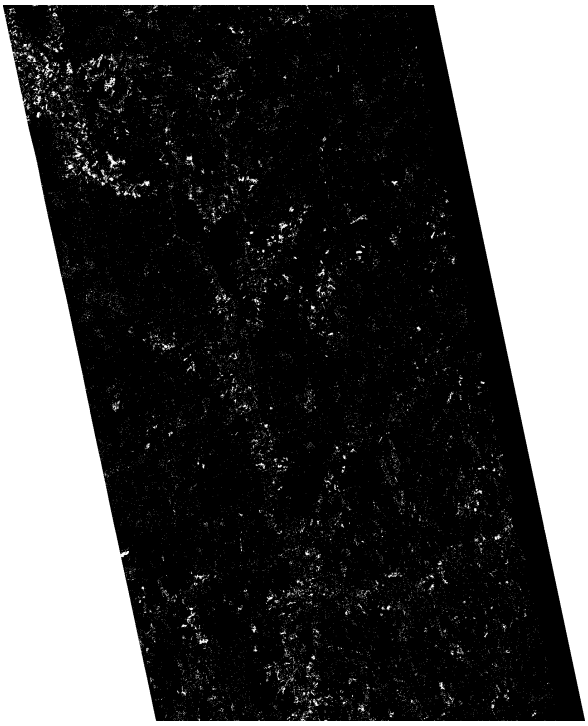

Fig. 3. Reference change image between March and May obtained with AutoChange on polarimetric PALSAR data

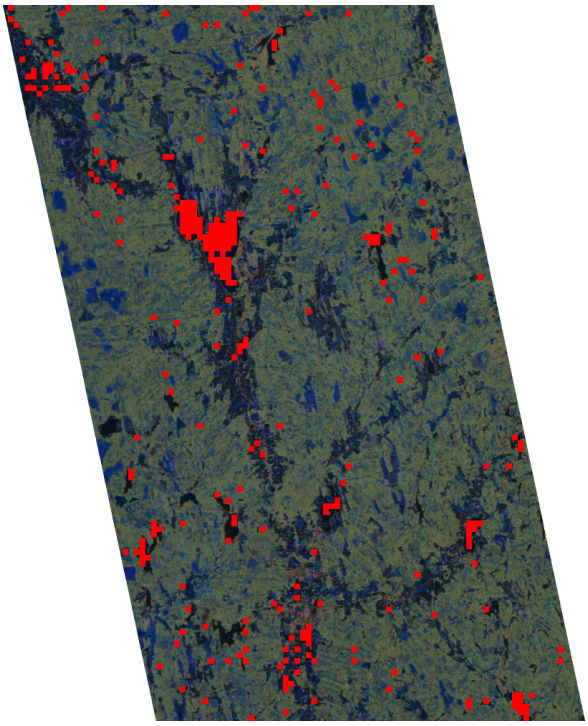

Fig. 4. 300 most relevant imagelets from all 25x20 histogram features (red squares), overlayed on May Pauli decomposition

sition of a satellite image into several thousands small images or imagelets, to generate an image database from which the user can query, visually and intuitively. Polarimetric feature groups were extracted and used to trained Self-Organising Maps. Various strategies for grouping pixel-wise features into feature groups were used, and the histogram approach turned out to improve results compared to simple pixel averaging. Improvements can be made in the polarimetric feature grouping strategy.

The same framework allows for detection of a specific content of interest, as well as change detection. The versatility of PicSOM will allow several applications to be embedded in a same operative and interactive system, only to be differentiated by the type of query. One of the many possible applications of this work is long term monitoring of human activity around strategic sites.

ACKNOWLEDGMENTS

This work was supported by the Academy of Finland in the projects *Neural methods in information retrieval based on automatic content analysis and relevance feedback* and *New information processing principles* (Finnish Centre of Excellence Programme 2006–2011), and *NewSAR*, funded by the Finnish Funding Agency for Technology and Innovation (TEKES.

REFERENCES

[1] Datcu, M., Daschiel, H., Pelizzari, A., Quartulli, M., Galoppo, A., Colapicchioni, A., Pastori, M., Seidel, K., Marchetti, P. G., and D'Elia, S. Information mining in remote sensing image archives - part A: System concepts. *IEEE Trans. Geoscience and Remote Sensing*, 41:2923–2936, December 2003.

[2] Healey, G. and Jain, A. Retrieving multispectral satellite images using physics-based invariant representation. *IEEE Trans. Pattern Analysis and Machine Intelligence*, 18:842–846, August 1996.

[3] Schröder, M., Seidel, K., and Datcu, M. User-oriented content labelling in remote sensing image archives. In *Proc. IEEE International Conference on Geoscience and Remote Sensing*, volume 2, pages 1019–1021, Seattle, USA, July 1998.

[4] Schröder, M., Rehrauer, H., Seidel, K., and Datcu, M. Interactive learning and probabilistic retrieval in remote sensing image archives. *IEEE Trans. Geoscience and Remote Sensing*, 38:2288–2298, September 2000.

[5] Seidel, K., Schröder, M., Rehrauer, H., and Datcu, M. Query by image content from remote sensing archives. In *Proc. IEEE Intern. Geoscience and Remote Sensing Symposium, IGARSS'98*, volume 1, pages 393–396, Seattle, USA, July 1998.

[6] Seidel, K. and Datcu, M. Architecture of a new generation of remote sensing ground segments. In *Proc. the 19th EARSeL Symposium on Remote Sensing in*

the 21st Century, pages 223–228, Valladolid, Spain, June 1999.

[7] Schröder, M. and Dimai, A. Texture information in remote sensing images: A case study. In *Workshop on Texture Analysis, WTA'98*, Freiburg, Germany, 1998.

[8] Schröder, M. Interactive learning in remote sensing image databases. In *Proc. IEEE Intern. Geoscience and Remote Sensing Symposium IGARSS'99*, 1999.

[9] Ferecatu, M., Boujemaa, N., and Crucianu, M. Active relevance feedback for interactive satellite images retrieval. In *Proc. ESA-EUSC Workshop on Image Information Mining - Theory and Application to Earth Observation*, Frascati, Italy, October 2005. ESA WPP-257 (Nov. 2005).

[10] Molinier, M., Laaksonen, J., and Häme, T. Detecting man-made structures and changes in satellite imagery with a content-based information retrieval system built on self-organizing maps. *IEEE Trans. Geoscience and Remote Sensing*, 45:861–874, April 2007.

[11] PicSOM Development Group. PicSOM online demonstration. http://www.cis.hut.fi/picsom, 1998–2008.

[12] Kohonen, T. *Self-Organizing Maps*, volume 30 of *Springer Series in Information Sciences*. Springer-Verlag, third edition, 2001.

[13] Laaksonen, J., Koskela, M., Laakso, S., and Oja, E. Self-organizing maps as a relevance feedback technique in content-based image retrieval. *Pattern Analysis & Applications*, 4(2+3):140–152, June 2001.

[14] Laaksonen, J., Koskela, M., and Oja, E. PicSOM—Self-organizing image retrieval with MPEG-7 content descriptions. *IEEE Transactions on Neural Networks, Special Issue on Intelligent Multimedia Processing*, 13(4):841–853, July 2002.

[15] Molinier, M., Laaksonen, J., Ahola, J., and Häme, T. Self-organizing map application for retrieval of man-made structures in remote sensing data. In *Proc. ESA-EUSC Workshop on Image Information Mining - Theory and Application to Earth Observation*, Frascati, Italy, October 2005. ESA WPP-257 (Nov. 2005).

[16] Lee, J.-S., Grunes, M. R., and De Grandi, G. Polarimetric sar speckle filtering and its implication for classification. *IEEE Transactions on Geoscience and Remote Sensing*, 37(5):2363–2373, September 1999.

[17] Lönnqvist, A., Rauste, Y., Ahola, H., Molinier, M., and Häme, T. Evaluation of classification methods with polarimetric alos/palsar data. In *Forests and Remote Sensing: Methods and Operational Tools (Forestsat 2007)*, Montpellier, France, 5-7 Nov. 2007.

[18] Molinier, M., Laaksonen, J., Rauste, Y., and Häme, T. Detecting changes in polarimetric sar data with content-based image retrieval. In *IEEE International Geoscience and Remote Sensing Symposium IGARSS'07, Barcelona, Spain*, pages 2390–2393, 23-28 July 2007.

[19] Pottier, E., Ferro-Famil, L., Allain, S., Cloude, S., Hajnsek, I., Papathanassiou, K., Moreira, A., Williams, M., Pearson, T., and Desnos, Y.-L. An overview of the PolSARpro v2.0 software. the educational toolbox for polarimetric and interferometric polarimetric SAR data processing. In *POLinSAR07 ESA Workshop*, January 2007.

[20] Häme, T., Heiler, I., and San Miguel-Ayanz, J. An unsupervised change detection and recognition system for forestry. *International Journal of Remote Sensing*, 19(6):1079–1099, April 1998.

[21] Laaksonen, J., Koskela, M., and Oja, E. Class distributions on SOM surfaces for feature extraction and object retrieval. *Neural Networks*, 17(8-9):1121–1133, October-November 2004.

[22] Dierking, W., Skriver, H., and Gudmandsen, P. SAR polarimetry for sea ice classification. In *Workshop on POLinSAR - Applications of SAR Polarimetry and Polarimetric Interferometry (ESA SP-529)*, January 2003.

[23] Skriver, H., Dierking, W., Gudmandsen, P., Toan, T. L., Moreira, A., Papathanassiou, K., and Quegan, S. Applications of synthetic aperture radar polarimetry. In *Workshop on POLinSAR - Applications of SAR Polarimetry and Polarimetric Interferometry (ESA SP-529)*, January 2003.

[24] Quegan, S., Le Toan, T., Skriver, H., Gomez-Dans, J., Gonzalez-Sampedro, M. C., and Hoekman, D. H. Crop classification with multitemporal polarimetric SAR data. In *Workshop on POLinSAR - Applications of SAR Polarimetry and Polarimetric Interferometry (ESA SP-529)*, January 2003.

[25] Buckley, J. R. Environmental change detection in prairie landscapes with simulated RADARSAT 2 imagery. In *IEEE International Geoscience and Remote Sensing Symposium IGARSS'02*, pages 3255–3257, 2002.

[26] Cloude, S. and Pottier, E. An entropy based classification scheme for land applications of polarimetric SAR. *IEEE Transactions on Geoscience and Remote Sensing*, 35(1):68–78, January 1997.

[27] Touzi, R., Goze, S., Toan, T. L., Lopes, A., and Mougin, E. Polarimetric discriminators for SAR images. *IEEE Transactions on Geoscience and Remote Sensing*, 30(5):973–980, September 1992.